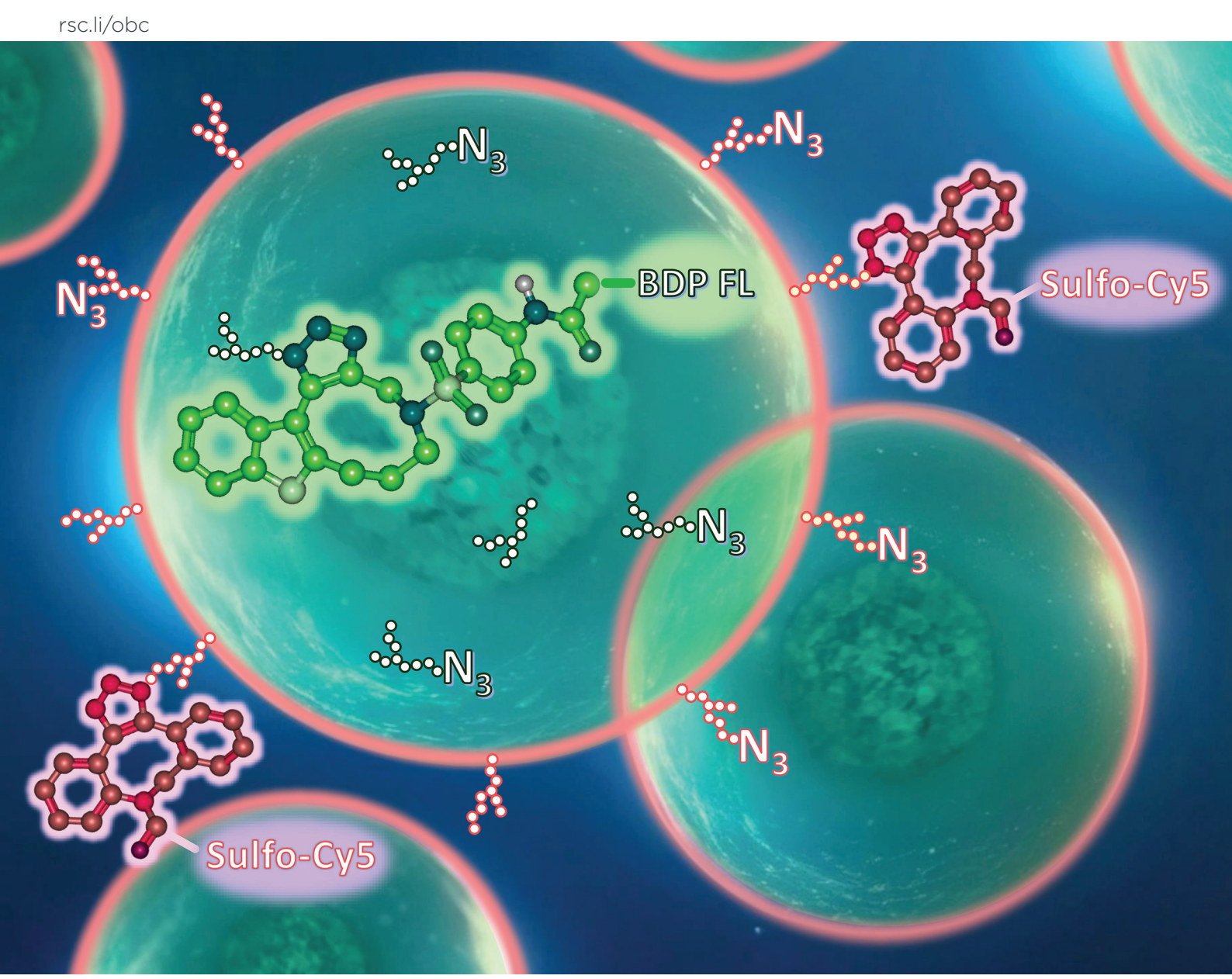
Volume 22 Number 37 7 October 2024 Pages 7527-7744

Organic & Biomolecular Chemistry



ISSN 1477-0520



PAPER

Stefan Bräse, Natalia A. Danilkina *et al.*Key role of cycloalkyne nature in alkyne-dye reagents for enhanced specificity of intracellular imaging by bioorthogonal bioconjugation

Organic & Biomolecular Chemistry



PAPER

View Article Online



Cite this: *Org. Biomol. Chem.*, 2024, **22**, 7637

Key role of cycloalkyne nature in alkyne-dye reagents for enhanced specificity of intracellular imaging by bioorthogonal bioconjugation†‡

Alexandra A. Vidyakina, D^a Sergey A. Silonov, D^{a,b} Anastasia I. Govdi, D^a Alexander Yu. Ivanov, D^c Ekaterina P. Podolskaya, Irina A. Balova, D^a Stefan Bräse D*^{e,f} and Natalia A. Danilkina D*^a

Received 20th June 2024, Accepted 2nd July 2024 DOI: 10.1039/d4ob01032a

rsc.li/obc

Conjugates of benzothiophene-fused azacyclononyne BT9N-NH₂ with fluorescent dyes were developed to visualise azidoglycans intracellularly. The significance of the cycloalkyne core was demonstrated by comparing new reagents with DBCO- and BCN-dye conjugates. To reduce non-specificity during intracellular bioconjugation using SPAAC, less reactive BT9N-dye reagents are preferred over highly reactive DBCO- and BCN-dye conjugates.

Bioorthogonal chemistry¹ is a modern field of research that aims to study complex biological systems using organic reactions, which do not interfere with biosystems and are not influenced by them.^{2,3} These bioorthogonal click reactions have a wide range of applications.^{4–8} Strain-promoted azide–alkyne cycloaddition (SPAAC) is one of the most widely used bioorthogonal transformations.^{9–12} SPAAC has been used to study cell-surface glycosylation,¹³ receptors engineering,¹⁴ to design therapeutic proteins, *e.g.*, lysosome-targeting chimeras¹⁵ and anticancer immunobiologicals.¹⁶ Nowadays, SPAAC is a common tool for visualising biomolecules,^{17–19} such as proteins,^{20,21} glycans,^{22,23} and nucleic acids²⁴ through fluorescent labelling *in vitro* and *in vivo*.²⁵

SPAAC visualisation typically involves two steps. The first step is aimed at incorporating azido groups into the biosystem either through metabolic labelling, ²⁶ *i.e.*, cell culturing in the

presence of unnatural azido monomers, or using organic azides with "directing" groups for specific organelles, such as mitochondria, lysosomes, Golgi apparatus, without metabolic incorporation into biopolymers. 27,28 The second step involves the SPAAC reaction between the N_3 -containing cell compartments and a cycloalkyne reagent conjugated with a fluorescent dve.

Depending on the studied N₃-labelled biological target, the cycloalkyne dye reagent should be able to reach the desired cell compartments. When labelling cell surface glycoproteins, it is important to use SPAAC active cycloalkyne reagents that cannot penetrate the cell membrane well to avoid nonspecific intracellular interactions. A dye with polar anionic groups, *e.g.*, from the sulfocyanine family, should be attached to the reactive cycloalkyne core to achieve this property. ^{23,29} To study intracellular N₃-labelled biomolecules, the reagent must effectively penetrate the cell membrane. ^{30,31} To achieve this, a lipophilic dye component without any polar anionic groups, commonly different BODIPY derivatives, or other ³² should be conjugated with the alkyne. Therefore, nowadays, different companies offer several SPAAC reagents conjugated to dyes of different natures.

Although a wide variety of cycloalkynes with different SPAAC reactivity and other properties have been developed, ^{33–36} the cycloalkyne nature is often overlooked and not taken into account in the case of intracellular biovisualisation. The choice of alkyne moieties in the commercially available cycloalkyne-dye reagents is limited to the most commonly used commercial conjugates with highly SPAAC-reactive **DBCO** (ADIBO, DIBAC)³⁷ or BCN³⁸ cycloalkyne scaffolds (Fig. 1A), which were originally developed as cell-surface labelling reagents.

^aInstitute of Chemistry, Saint Petersburg State University (SPbU), Saint Petersburg, 199034, Russia. E-mail: n.danilkina@spbu.ru

^bLaboratory of Structural Dynamics, Stability and Folding of Proteins, Institute of Cytology, Russian Academy of Sciences, 194064, Russia

^cCenter for Magnetic Resonance, Research Park, Saint Petersburg State University (SPbU), Saint Petersburg, 199034, Russia

^dInstitute of Analytical Instrumentation RAS, 190103 St. Petersburg, Russia ^eInstitute of Organic Chemistry (IOC), Karlsruhe Institute of Technology (KIT), 76131 Karlsruhe, Germany. E-mail: stefan.braese@kit.edu

^fInstitute of Biological and Chemical Systems – Functional Molecular Systems (IBCS-FMS), Karlsruhe Institute of Technology (KIT), 76344 Eggenstein-Leopoldshafen, Germany

[†]Dedicated to the 300th anniversary of the Saint Petersburg University foundation.

[‡] Electronic supplementary information (ESI) available: All synthetic and biological details, copies of NMR spectra. See DOI: https://doi.org/10.1039/d4ob01032a

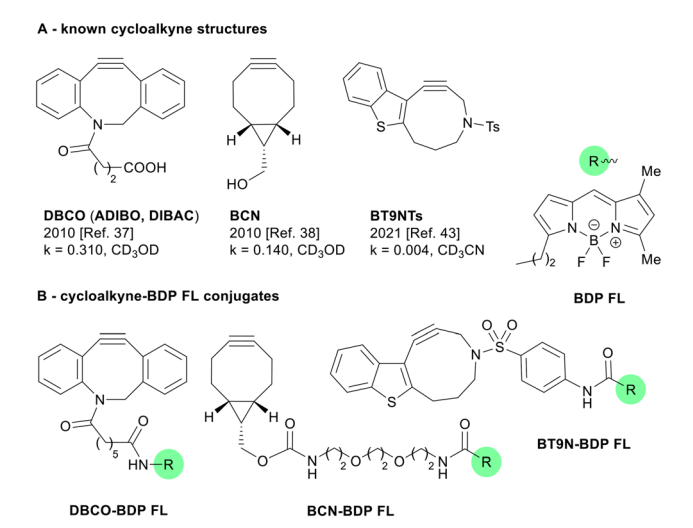


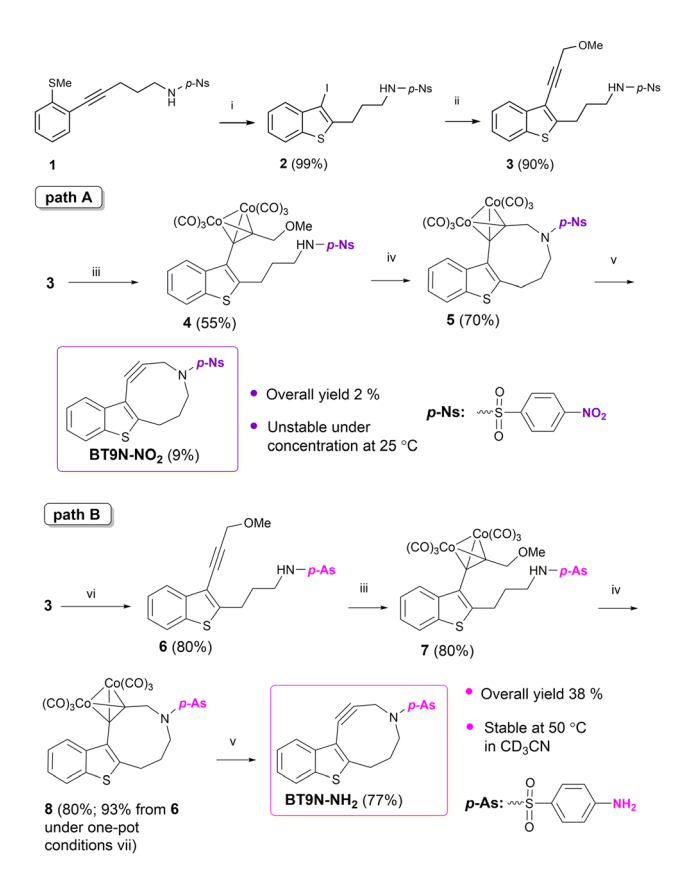
Fig. 1 Structures of known DBCO- and BCN-based BDP FL reagents and new BT9N-BDP FL dye conjugates studied in this work; k – SPAAC rate constant for BnN₃, M⁻¹ s⁻¹.

However, neglecting the cycloalkane nature, especially when intracellular staining of metabolically labelled compartments is involved, can lead to a high nonspecific fluorescence response due to the known reactivity of BCN and DBCO towards thiols (such as cysteine residues and glutathione)³⁹ and sulfenic acids, 40-42 which are common in biosystems.

Therefore, here we study the development of new reagents for efficient intracellular labelling, paying major attention to the cycloalkyne's nature. We synthesized a cycloalkyne-BODIPY-FL conjugate BT9N-BDP FL (Fig. 1B), an analogue of BT9NTs⁴³ (Fig. 1A), and compare its efficiency and specificity for the intracellular labelling with other BODIPY-FL cycloalkyne reagents having more reactive in SPAAC DBCO and BCN alkyne cores (Fig. 1B). We demonstrated that for the visualisation of intracellular N₃-glycoconjugates the nature of cycloalkyne is dramatically important. The designed BT9N-BDP FL reagent and its triazole-conjugated analogue BT9N-Tr have an advantage over DBCO-BDP FL and BCN-BDP FL, which showed significantly higher nonspecific affinity towards the intracellular environment.

The prototype of the BT9N-BDP FL conjugate is the BT9NTs cycloalkyne from heterocycle-fused heterocycloalkyne family (Fig. 1), which has been discovered recently 43,44 using a combination of the "reagent destabilisation" and the "SPAAC transition state stabilisation" approaches. 11 BT9NTs possess the highest SPAAC reactivity within this group, but it is unsuitable for conjugation with a dye because the molecule lacks any reactive functionalities. To synthesise the BT9N-BDP FL conjugate, we decide to replace the Ts group with 4-aminobenzenesulfonamide (As) moiety and use the NH2 group of BT9N-NH2 as a site for functionalisation with a BDP FL dye.

The starting material chosen was 4-nitro-N-(pent-4-yn-1-yl) benzenesulfonamide (S1). The synthetic route for BT9N-NH2 is similar to that for BT9NTs43 and consists of three main



Scheme 1 Optimisation of the synthetic procedure of BT9N-NH₂. Reagents and conditions: (i) I2, DCM, r.t., 1 h; (ii) methyl propargyl ether, Pd(PPh₃)₄ (5.00 mol%), CuI (15.0 mol%), KF, DMF, 50 °C, 3 h; (iii) $Co_2(CO)_8$, benzene, c = 0.01 M, r.t., 2-3 h; (iv) $BF_3 \cdot OEt_2$, DCM, c = 0.001M, 0 °C to r.t., 2 h; (v) TBAF·H₂O acetone/H₂O (15:1), c = 0.006 M, r.t., 4-5 h; (vi) Fe powder, NH₄Cl, acetone/H₂O (1:1), 40 °C, 48 h; (vii) Cocomplexation/Nicholas reaction in one-pot: Co₂(CO)₈ DCM = 0.01 M, r. t., 2 h, then BF_3 ·OEt₂, DCM, c = 0.0035 M, 0 °C to r.t., 15 min.

steps: the Sonogashira cross-coupling, electrophile-promoted cyclisation and the Nicholas cyclisation (Scheme 1). The main question was at what stage the nitro group should be reduced. First, we decided to reduce NO2 at the last stage under conditions that tolerated up to a triple bond⁴⁵ and obtain the nitroalkyne BT9N-NO2 via pathway A (Scheme 1, path A). However, due to its instability, the cycloalkyne BT9N-NO2 without the Co-protecting group was only isolated in a 9% yield. To overcome this problem, we moved the NO₂ reduction step to an earlier stage and tried the Nicholas cyclisation for the NH2 derivative 7 (Scheme 1, path B). Although the Nicholas reaction for NH2-containing compounds does not go well, 46 to our delight, this reaction for the amino Co-complex 7 gave the desired cyclic product 8 in high yield without forming any by-products. Complex 8 can be obtained even in higher yield using Co-complexation/ Nicholas cyclisation in one pot. Cycloalkyne BT9N-NH₂ obtained by deprotection of complex 8 showed excellent stability under isolation, storage and heating at 50 °C for 24 hours in CD₃CN.

We then turned to the synthesis of the BT9N-BDP FL conjugate. However, 4-aminobenzenesulfonamide moiety was inert towards electrophilic agents, e.g. isothiocyanates, anhydrides and carboxylic acids with coupling reagents (ESI, section 2.3‡). Finally, we found that BT9N-NH2 could be modified by acylation with acetyl chloride (ESI, 2.3.21). Therefore, BDP FL acid chloride⁴⁷ was used to synthesise BT9N-BDP FL under optimised conditions (Scheme 2) (ESI, section 2.2‡).

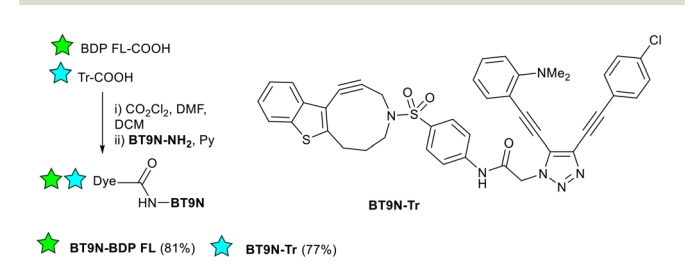
The synthesis of another example of the BT9N SPAAC reagent, BT9N-Tr (Scheme 2), followed the same procedure. This reagent was examined as an additional BT9N-dye conjugate with a non-commercial lypophilic dye belonging to a pullpush triazole family. 48 This would demonstrate the importance of the cycloalkyne nature for intracellular biovisualisation, irrespective of a lipophilic dye core. BCN-BDP FL was synthesised using commercially available BCN-NH2 and BDP FL NHS ester (ESI, section 2.2‡). The DBCO-BDP FL conjugate was obtained from Lumiprobe, a commercial supplier.

Using four different cycloalkyne reagents (BT9N-BDP FL, BT9N-Tr, BCN-BDP FL and DBCO-BDP FL), we performed biological studies to demonstrate the importance of the cycloalkyne core in the intracellular visualisation of metabolically labelled azido glycans. Before the studies, the cytotoxicity of all compounds was evaluated using HeLa and HEK293 cell lines (ESI, Fig. S1[†]). All reagents were nontoxic under concentration of 1 μ M, which was used for all further bioimaging assays.

Three different azidosugars were studied: Ac₄ManNAz (tetraacetylated N-azidoacetyl-mannosamine) was used as a sugar known to be the component of sialic acid found on the cell surface, Ac₄GalNAz (tetraacetylated N-azidoacetyl-galactosamine) was used a source of mucin O-linked glycosylation for both cell surface and intracellular glycans and Ac₄GlcNAz (tetraacetylated N-azidoacetyl-glucosamine) was used for mostly intracellular labelling. 13,27,49

HeLa cells were treated with the corresponding acylated N₃sugar for 72 hours. Subsequently, they were stained with the corresponding cycloalkyne-dye conjugate for 4 hours (Fig. 2A). To control the distribution of each azidosugar on the cell surface, two DBCO reagents were used: one conjugated with fluorescein dye (DBCO-F) and the other with Sulfocyanine 5 dye (DBCO-SCy5) (Fig. 2B and C).

The data obtained revealed that both BT9N-dye conjugates, BT9N-BDP FL and BT9N-Tr, demonstrate significantly higher specificity in N3-dependent intracellular labelling of



Scheme 2 Synthesis of BT9N-Dye conjugates.

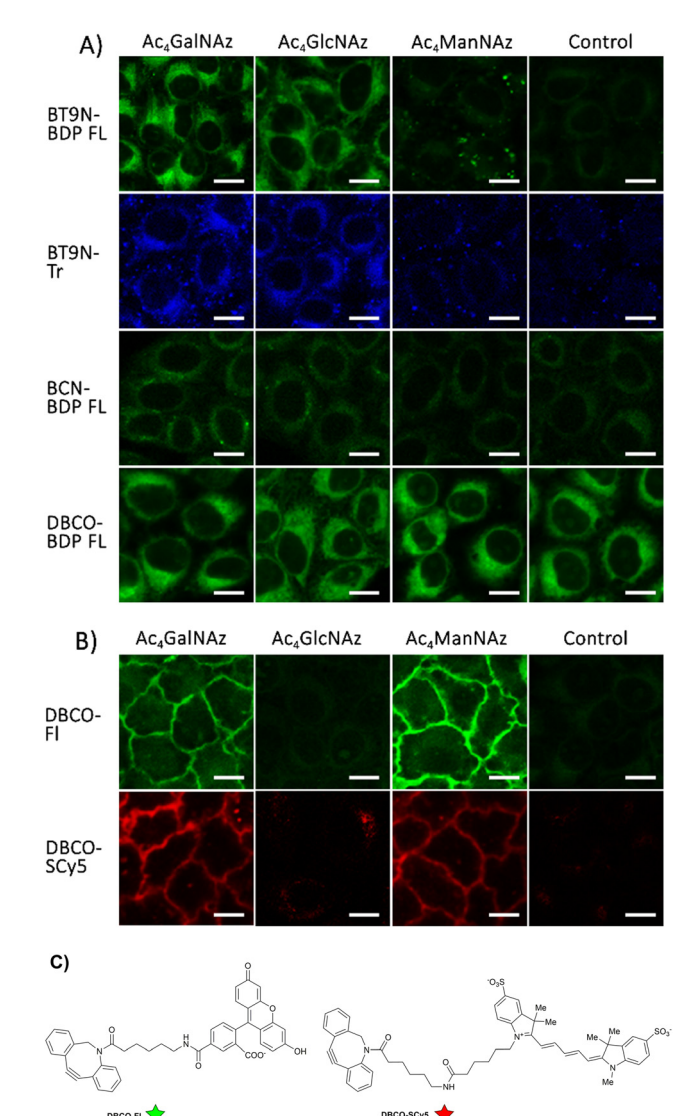


Fig. 2 Confocal fluorescent imaging of HeLa cells treated with the corresponding sugars (50 µM, 72 h) and then incubated with the respective alkyne-dye conjugate (1 μM, 4 h) BT9N-BDP FL, BT9N-Tr, BCN-BDP FL, DBCO-BDP FL (A) and DBCO-Fl, DBCO-SCy5 (B); structures of DBCO-Fl and DBCO-SCy5 are represented in (C). Fluorescence images for BT9N-BDP FL, BCN-BDP FL, DBCO-BDP FL, and DBCO-Fl conjugates were captured using the FITC channel (Ex. 488 nm, Em. 500-550 nm); for BT9N-Tr, the DAPI channel was used (Ex. 406 nm. Em. 425-475 nm); for DBCO-SCy5, the Cy5 channel was used (Ex. 638 nm, Em. 663-738 nm)-scale bar: 15 μm.

Ac₄GalNAz and Ac₄GlcNAz treated cells compared to BCN-BDP FL and DBCO-BDP FL. These two latter conjugates displayed serious nonspecific labelling in non-treated control cells (for a quantitative comparison of the fluorescent response, refer to the ESI, Fig. S2‡). Furthermore, only weak fluorescence was observed in Ac₄ManNAz metabolically labelled cells for both BT9N conjugates, which confirms the known cell-surface localisation of the deacylated mannosamine. The significantly stronger intracellular fluorescence observed in Ac₄ManNAz treated cells for BCN-BDP FL and DBCO-BDP FL is likely due

Paper

to the nonspecific binding of alkyne-dye conjugates with the intracellular environment.

It is interesting to note that **DBCO-BDP FL** exhibited greater nonspecific intracellular labelling compared to **BCN-BDP FL**, which is consistent with the general reactivity of **DBCO**. ^{37,50}

The nonspecific behaviour of **DBCO** and **BCN** reagents in cells is more likely due to their high reactivity not only in SPAAC but also with other "alkynophiles" present in the biological environment, such as the –SH and –SOH groups of proteins.

Thus it has been shown, that **BCN** and **DBCO** can react with peptidylcysteines, which is the reason of azide-independent labeling and that it can be diminished by iodoacetamide alkylation of thioles.³⁹ Moreover the reactivity of BCN and DBCO towards sulfenic acids has been also proved.^{40–42}

We have recently reported that the prototype of BT9N-based dyes, a cycloalkyne BT9NTs, does not react with t-BuSH in CD₃CN even at 37 °C for 24 h. 43 To demonstrate that cycloalkvne-dve reagents BT9N-BDP FL and BT9N-Tr are less reactive than DBCO and BCN dyes towards SH-containing biospecies, we conducted a study investigating the behavior of all four compounds towards glutathione (GSH) and human globin using MALDI TOF mass spectrometry (for details see ESI, section 5‡).⁵¹ It was estimated that **DBCO** and **BCN** dyes form adducts with human globin (alpha and beta subunits) after 3 hours of incubation at 37 $^{\circ}$ C (pH = 7.2), while **BT9N**-dyes do not react with the protein. Furthermore, we identified monoand bis-adducts of DBCO and a monoadduct of BCN with GSH using 2,5-dihydroxybenzoic acid (DHB) and α-cyano-4-hydroxycinnamic acid (CHCA) as a matrix for MALDI spectra. In the case of BT9N-BDP FL, only a monoadduct was identified using the DHB matrix, whereas no adducts were observed for BT9N-Tr in both matrices. Therefore, our findings indicate that less SPAAC reactive cycloalkyne-dye conjugates, based on BT9N, display increased tolerance towards endogenous thiol species in comparison with more active DBCO and BCN derivatives.

To demonstrate the pivotal role of selecting of the optimal cycloalkyne as a component of a cycloalkyne-dye reagent in achieving the desired outcomes of a study, we conducted double labelling experiments (Fig. 3).

In order to label intracellular and cell surface glycans in a single metabolic labelling experiment, either Ac₄GalNAz or both Ac₄ManNAz and Ac₄GlcNAz were employed in the metabolic labelling of HeLa (Fig. 3A) and HEK293 (Fig. 3B) cell lines. BT9N-BDP FL and DBCO-SCy5 were used in order to simultaneously visualise intracellular and surface N₃-glycans in green and red channels, respectively. The merged images for both cell lines in every case demonstrated that BT9N-BDP FL is an effective reagent for visualising intracellular azidoglycans (N₃-glucose and intracellular N₃-galactose), while DBCO-SCy5 is a reagent of choice for visualising cell surface glycans (N₃-mannose and cell surface N₃-galactose). It is of paramount importance that both reagents act orthogonally and can be employed for the labelling of corresponding glycans during a single double-labelling experiment.

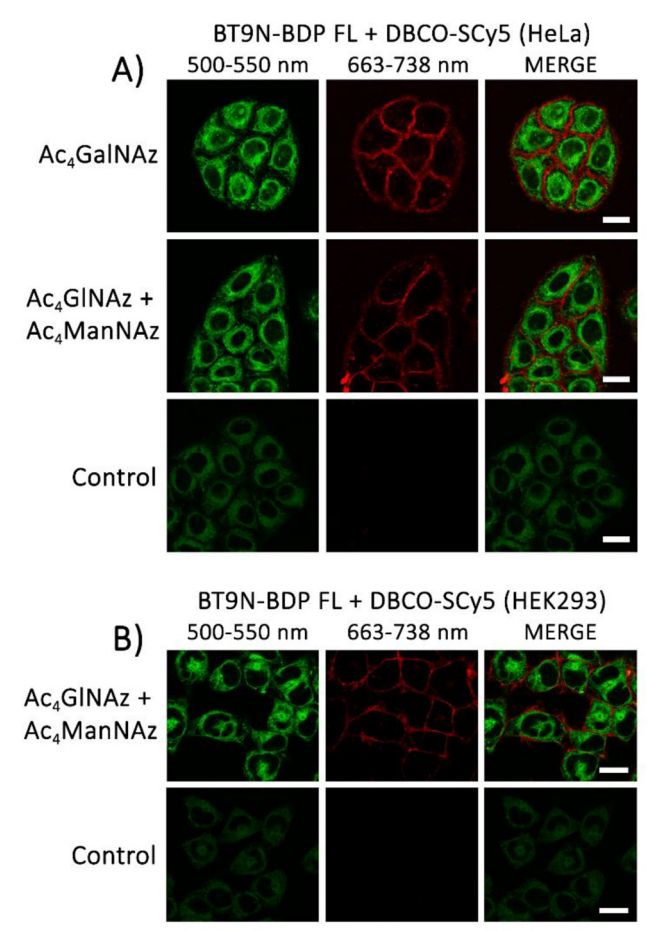


Fig. 3 Confocal fluorescent imaging of HeLa (A) and Hek293 (B) cells treated with the corresponding sugars (50 $\mu\text{M},$ 72 h) and then incubated first with BT9N-BDP FL (1 $\mu\text{M},$ 3 h), and then with DBCO-SCy5 (1 $\mu\text{M},$ 30 min) for double intracellular and cell surface labelling, respectively. Fluorescence images for BT9N-BDP FL conjugates were captured using the FITC channel (Ex. 488 nm, Em. 500–550 nm); for DBCO-SCy5, the Cy5 channel was used (Ex. 638 nm, Em. 663–738 nm)—scale bar: 20 $\mu\text{m}.$

Conclusions

Azacyclononyne dye conjugates BT9N-BDP FL, and BT9N-Tr have been developed for intracellular fluorescent labelling of N_3 -glycans containing cells. We have demonstrated the important role of the cycloalkyne core for intracellular bioimaging. Even though BT9N derivatives have significantly slower SPAAC kinetics with azides compared to the two well-known cyclooctynes (BCN and DBCO), we have shown that in the case of intracellular biorthogonal bioconjugation, this disadvantage turns into an advantage due to minimal nonspecific binding of BT9N derivatives with the intracellular bioenvironment.

Author contributions

AAV and SAS contributed equally to this work. AAV – investigation, methodology, writing – original draft; SAS – investi-

gation, methodology, visualisation; AIG – investigation; AYuI – formal analysis; EPP – investigation; IAB – project administration, supervision; SB – project administration, supervision, writing – review & editing; NAD – conceptualization, data curation, methodology, project administration, supervision, visualization, funding acquisition, writing – original draft, writing – review & editing.

Data availability

The data supporting this article have been included as part of the ESI‡: synthetic procedures, MTT test details, cell culture and confocal microscopy, MALDI TOF mass spectrometry details and copies of MS spectra, copies of NMR spectra of all synthesized compounds.

Conflicts of interest

There are no conflicts to declare.

Acknowledgements

This work was funded by the Russian Science Foundation 24-23-00377. The research was carried out using the SPbU Resource Centres: Magnetic Resonance Research Centre, Chemical Analysis and Materials Research Centre, Centre for Optical and Laser Materials Research, Center for Molecular and Cell Technologies; Oussama Abdelhamid Mammeri (SPbU) is thanked for ESI HR MS measurements.

References

- 1 J. A. Prescher and C. R. Bertozzi, *Nat. Chem. Biol.*, 2005, 1, 13–21.
- 2 T. Deb, J. Tu and R. M. Franzini, *Chem. Rev.*, 2021, **121**, 6850-6914.
- 3 S. S. Nguyen and J. A. Prescher, *Nat. Rev. Chem.*, 2020, 4, 476–489.
- 4 C. Pan, X. Jiang, C. Liu, J. Wei, Y. Wang, C. Yang and Y. Gan, *Chem. Eng. J.*, 2024, **480**, 148120.
- 5 R. E. Bird, S. A. Lemmel, X. Yu and Q. A. Zhou, *Bioconjugate Chem.*, 2021, 32, 2457–2479.
- 6 Q. Zhang, G. Kuang, L. Wang, P. Duan, W. Sun and F. Ye, *Research*, 2023, **6**, 1–26.
- 7 E. Kim and H. Koo, Chem. Sci., 2019, 10, 7835-7851.
- 8 W. Yi, P. Xiao, X. Liu, Z. Zhao, X. Sun, J. Wang, L. Zhou, G. Wang, H. Cao, D. Wang and Y. Li, *Signal Transduction Targeted Ther.*, 2022, 7, 386.
- 9 N. J. Agard, J. A. Prescher and C. R. Bertozzi, *J. Am. Chem. Soc.*, 2004, **126**, 15046–15047.
- 10 E. G. Chupakhin and M. Y. Krasavin, *Chem. Heterocycl. Compd.*, 2018, **54**, 483–501.

- 11 T. Harris and I. V. Alabugin, *Mendeleev Commun.*, 2019, 29, 237–248.
- 12 J. Dommerholt, F. P. J. T. Rutjes and F. L. van Delft, *Top. Curr. Chem.*, 2016, 374, 16.
- 13 H. Xiao, G. X. Tang and R. Wu, Anal. Chem., 2016, 88, 3324-3332.
- 14 C.-H. Lee, S. Park, S. Kim, J. Y. Hyun, H. S. Lee and I. Shin, *Chem. Sci.*, 2024, **15**, 555–565.
- 15 S. M. Banik, K. Pedram, S. Wisnovsky, G. Ahn, N. M. Riley and C. R. Bertozzi, *Nature*, 2020, 584, 291–297.
- 16 P. A. Szijj, M. A. Gray, M. K. Ribi, C. Bahou, J. C. F. Nogueira, C. R. Bertozzi and V. Chudasama, *Nat. Chem.*, 2023, **15**, 1636–1647.
- 17 E. Kozma and P. Kele, Top. Curr. Chem., 2024, 382, 7.
- 18 G. B. Cserép, A. Herner and P. Kele, *Methods Appl. Fluoresc.*, 2015, 3, 042001.
- 19 S. H. Alamudi, X. Liu and Y.-T. Chang, *Biophys. Rev.*, 2021, 2, 021301.
- 20 S. H. Alamudi, R. Satapathy, J. Kim, D. Su, H. Ren, R. Das, L. Hu, E. Alvarado-Martínez, J. Y. Lee, C. Hoppmann, E. Peña-Cabrera, H.-H. Ha, H.-S. Park, L. Wang and Y.-T. Chang, *Nat. Commun.*, 2016, 7, 11964.
- 21 P. Mateos-Gil, S. Letschert, S. Doose and M. Sauer, Front. Cell Dev. Biol., 2016, 4, 1–16.
- 22 X. Wen, B. Yuan, J. Zhang, X. Meng, Q. Guo, L. Li, Z. Li, H. Jiang and K. Wang, *Chem. Commun.*, 2019, 55, 6114–6117.
- 23 S. K. Leong, Y. Chen, J. Hsiao, C. Tsai and J. Shie, *ChemBioChem*, 2023, 24, 1–7.
- 24 J. Zayas, M. Annoual, J. K. Das, Q. Felty, W. G. Gonzalez, J. Miksovska, N. Sharifai, A. Chiba and S. F. Wnuk, *Bioconjugate Chem.*, 2015, 26, 1519–1532.
- 25 D. Chen, Y. Lin, A. Li, X. Luo, C. Yang, J. Gao and H. Lin, *Anal. Chem.*, 2022, **94**, 16614–16621.
- 26 K. Dammen-Brower, E. Tan, R. T. Almaraz, J. Du and K. J. Yarema, *Curr. Protoc.*, 2023, 3, e822.
- 27 S. H. Alamudi, D. Su, K. J. Lee, J. Y. Lee, J. L. Belmonte-Vázquez, H.-S. Park, E. Peña-Cabrera and Y.-T. Chang, *Chem. Sci.*, 2018, **9**, 2376–2383.
- 28 M. Xiao, Y. Zhang, R. Li, S. Li, D. Wang and P. An, *Chem. Asian J.*, 2022, **17**, e202200634.
- 29 H. Stöckmann, A. A. Neves, S. Stairs, H. Ireland-Zecchini, K. M. Brindle and F. J. Leeper, *Chem. Sci.*, 2011, 2, 932.
- 30 V. Šlachtová, M. Chovanec, M. Rahm and M. Vrabel, *Top. Curr. Chem.*, 2024, 382, 2.
- 31 V. Rigolot, C. Biot and C. Lion, *Angew. Chem., Int. Ed.*, 2021, **60**, 23084–23105.
- 32 S. H. Alamudi and Y.-T. Chang, *Chem. Commun.*, 2018, 54, 13641–13653.
- 33 Y. Hu, R. Spiegelhoff, K. S. Lee, K. M. Sanders and J. M. Schomaker, *J. Org. Chem.*, 2024, **89**, 4512–4522.
- 34 E. Das, M. A. M. Feliciano, P. Yamanushkin, X. Lin and B. Gold, *Org. Biomol. Chem.*, 2023, **21**, 8857–8862.
- 35 M. J. Holzmann, N. Khanal, P. Yamanushkin and B. Gold, *Org. Lett.*, 2023, 25, 309–313.

- 36 J. Weterings, C. J. F. Rijcken, H. Veldhuis, T. Meulemans, D. Hadavi, M. Timmers, M. Honing, H. Ippel and R. M. J. Liskamp, *Chem. Sci.*, 2020, 11, 9011–9016.
- 37 M. F. Debets, S. S. van Berkel, S. Schoffelen, F. P. J. T. Rutjes, J. C. M. van Hest and F. L. van Delft, *Chem. Commun.*, 2010, **46**, 97–99.
- 38 J. Dommerholt, S. Schmidt, R. Temming, L. J. A. Hendriks, F. P. J. T. Rutjes, J. C. M. van Hest, D. J. Lefeber, P. Friedl and F. L. van Delft, Angew. Chem., Int. Ed., 2010, 49, 9422–9425.
- 39 R. van Geel, G. J. M. Pruijn, F. L. van Delft and W. C. Boelens, *Bioconjugate Chem.*, 2012, 23, 392–398.
- 40 T. H. Poole, J. A. Reisz, W. Zhao, L. B. Poole, C. M. Furdui and S. B. King, *J. Am. Chem. Soc.*, 2014, **136**, 6167–6170.
- 41 Z. Li, T. E. Forshaw, R. J. Holmila, S. A. Vance, H. Wu, L. B. Poole, C. M. Furdui and S. B. King, *Chem. Res. Toxicol.*, 2019, 32, 526–534.
- 42 D. J. McGarry, M. M. Shchepinova, S. Lilla, R. C. Hartley and M. F. Olson, ACS Chem. Biol., 2016, 11, 3300–3304.
- 43 N. A. Danilkina, A. I. Govdi, A. F. Khlebnikov, A. O. Tikhomirov, V. V. Sharoyko, A. A. Shtyrov, M. N. Ryazantsev, S. Bräse and I. A. Balova, *J. Am. Chem. Soc.*, 2021, 143, 16519–16537.

- 44 A. A. Vidyakina, A. A. Shtyrov, M. N. Ryazantsev,
 A. F. Khlebnikov, I. E. Kolesnikov, V. V. Sharoyko,
 D. V. Spiridonova, I. A. Balova, S. Bräse and
 N. A. Danilkina, *Chem. Eur. J.*, 2023, 29, e202300540.
- 45 K. Kaneda, R. Naruse and S. Yamamoto, *Org. Lett.*, 2017, **19**, 1096–1099.
- 46 N. A. Danilkina, E. A. Khmelevskaya, A. G. Lyapunova, A. S. D'Yachenko, A. S. Bunev, R. E. Gasanov, M. A. Gureev and I. A. Balova, *Molecules*, 2022, 27, 6071.
- 47 B. Brandes, S. Hoenke, L. Fischer and R. Csuk, *Eur. J. Med. Chem.*, 2020, **185**, 111858.
- 48 A. I. Govdi, P. V. Tokareva, A. M. Rumyantsev, M. S. Panov, J. Stellmacher, U. Alexiev, N. A. Danilkina and I. A. Balova, *Molecules*, 2022, 27, 3191.
- 49 N. J. Pedowitz and M. R. Pratt, RSC Chem. Biol., 2021, 2, 306-321.
- C. Zhang, P. Dai, A. A. Vinogradov, Z. P. Gates and
 B. L. Pentelute, *Angew. Chem., Int. Ed.*, 2018, 57, 6459–6463.
- 51 A. Gorbunov, A. Bardin, S. Ilyushonok, J. Kovach, A. Petrenko, N. Sukhodolov, K. Krasnov, N. Krasnov, I. Zorin, A. Obornev, V. Babakov, A. Radilov and E. Podolskaya, *Microchem. J.*, 2022, 178, 107362.